THERMAL LOAD ANALYSIS AND CONTROL OF FOUR-STROKE HIGH SPEED DIESEL ENGINE

by

Zixu GUAN and Yi CUI *

Key Laboratory of Power Machinery and Engineering of Ministry of Education,
Shanghai Jiao Tong University, Shanghai, China

Original scientific paper
https://doi.org/10.2298/TSCI190915163G

Aiming at the thermal load problem of the four-stroke high-speed Diesel engine piston, a piston thermal fluid-solid coupling model based on the combustion thermal boundary and the two-phase flow oscillation cooling thermal boundary is established. The model considers the problem that the piston cannot fill the cooling cavity due to the reciprocating motion. The effects of different engine speeds and the injection speed on the filling rate are studied. The variation curves of the filling rate of the oil in the cooling cavity are simulated, and the transient heat transfer coefficient and temperature of each crank angle are obtained. The average value is then analyzed by thermal flow-solid coupling method, and the influence of the filling rate of the piston cavity on the temperature field of the piston is obtained. Through the comparison of the experimental results of the hardness plug measurement method, the calculation of the model is accurate and can be well used for the simulation of the piston temperature field and the evaluation of the thermal load at the critical position. Based on this model, the regularity analysis of the influencing factors of the piston thermal load is carried out. The influencing factors include the filling rate of the cavity, the air-fuel ratio, the injection timing, etc., and finally the engine operating range that meets the heat load requirements is obtained.

Key words: *filling rate, combustion-cooling coupling simulation, air-fuel ratio, injection timing, piston, oscillating heat transfer*

Introduction

The four-stroke high-speed Diesel engine studied in this paper needs to change the operating conditions and environment so that it can obtain greater power and fuel economy, thus causing changes in its thermal load. In order to ensure the operational reliability of the retrofit, it must be ensured that its thermal load does not exceed the operating limit of the piston thermal load. Therefore, based on the piston temperature field, the influence of various factors on the engine heat load is studied, and the relevant laws are summarized. Finally, the engine operable range that meets the heat load requirements is given.

The piston is subjected to a large thermal load and mechanical load during the operation of the engine. The top surface of the piston is in direct contact with the high temperature gas, and the heat dissipation condition of the piston is not good, which causes the high working temperature of the piston, thereby reducing the mechanical mechanism of the material and the resistance to deformation [1]. In addition, the lubrication condition of the piston

* Corresponding author, e-mail: ycui@sjtu.edu.cn

ring is also affected by the heat load. Generally, the temperature of the first ring groove must be lower than the glue temperature of the oil, otherwise the oil can be glued and the engine lubrication condition is deteriorated [2]. The thermal boundary conditions of the piston combustion chamber are mainly determined by the combustion factors. The air-fuel ratio and injection timing have a decisive influence on the heat released by the combustion. Therefore, the influence of these two factors on the thermal load of the piston is considered in this paper. The heat exchange of the piston mainly includes the heat exchange between the cylinder gas and the piston top, the heat exchange of the piston cooling inner cavity, and the heat exchange with the cylinder liner wall surface and the crankcase environment. The heat transfer in the cooling chamber is complex [3]. The reciprocating motion of the piston causes the cooling oil to fill the cooling chamber, so the oil reciprocates in the cooling chamber of the piston, which can bring better heat transfer effect [4]. This paper focuses on the analysis of the oil filling rate under different engine speeds and different cooling oil injection rates, and also the influence of filling rate on the cooling effect.

In this paper, the fluid-solid coupling simulation model of the combustion heat boundary and the two-phase flow oscillating heat transfer boundary is established firstly, so as to simulate the piston temperature field, and the simulation results are evaluated by the experimental results of the hardness plug measurement method to verify the method accurately. Based on the simulation method, combined with the engine working process simulation, the relationship among the air-fuel ratio in the cylinder, the injection timing, the oil filling rate and the engine heat load is analyzed. The engine operating range that meets the piston thermal load limit requirements is obtained and it can also provide a basis for engine performance improvement and optimization.

Heat fluid-solid coupling calculation model

The analysis object is a high-speed four-stroke Diesel engine piston. The piston has two cooling oil inlets as shown in fig. 1. The fixed oil injectors spray oil from the bottom to the inlet port with a certain injection flow rate.

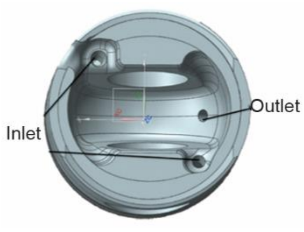

Figure 1. Schematic diagram of the piston

A solid finite element calculation model is established for the aluminum alloy piston, and a CFD two-phase flow calculation model is established for the cooling cavity of the piston. The finite element for temperature field analysis is the tetrahedral second-order mesh, shown in fig. 2. The element of the inner cavity is the prismatic layer mesh, as shown in fig. 3.

First, the gas thermal boundary conditions are analyzed. The heat releasing from the inner wall of the combustion chamber in the case of stable operation of the Diesel engine varies with time and space, but it changes periodically for each working cycle. Therefore, the heat transfer amount of the gas to the wall surface in one cycle can be calculated by:

$$q = \frac{1}{\tau_0} \int_0^{\tau_0} h_g (T_g - t_{w,s}) \mathrm{d}\tau \tag{1}$$

where τ_0 is the period of a working cycle, h_g – the transient heat transfer coefficient of the gas, T_g – the instantaneous temperature of the gas, $t_{w,s}$ – the instantaneous temperature of the top surface, and q – the heat transfer from gas to wall.

Figure 2. Piston mesh model

Figure 3. Piston cooling cavity mesh model

Generally, the wall temperature change within a cycle is not large, and its temperature is much lower than the gas temperature, so it can be taken as an average value T_{wm}. And then q can also be calculated by:

$$q=\frac{1}{\tau_0}\int_0^{\tau_0} h_{\mathrm{g}}T_{\mathrm{g}}\mathrm{d}\tau - T_{\mathrm{wm}}\frac{1}{\tau_0}\int_0^{\tau_0} h_{\mathrm{g}}\mathrm{d}\tau = h_{\mathrm{gm}}(T_{\mathrm{res}}-T_{\mathrm{wm}}) \tag{2}$$

where T_{res} is the equivalent average gas temperature based on heat flow and h_{gm} is the average heat transfer coefficient.

$$T_{\mathrm{res}}=\frac{(h_{\mathrm{g}}T_{\mathrm{g}})_{\mathrm{m}}}{h_{\mathrm{gm}}} \tag{3}$$

It can be seen from eq. (3) that the required equivalent average gas temperature T_{res} and the average heat transfer coefficient h_{gm} must first start from the instantaneous gas temperature, T_{g}, and the instantaneous heat transfer coefficient, h_{g}, in the cylinder.

From the perspective of heat transfer, the heat transfer coefficient is related to many factors. It is very difficult to theoretically solve it by analytical methods. Generally, some empirical and semi-empirical formulas are used to determine the instantaneous heat transfer coefficient, h_{g}, of gas. This paper uses the Eickelberg formula to calculate:

$$h_{\mathrm{g}}=7.8(C_{\mathrm{m}})^{1/3}(p_{\mathrm{g}}T_{\mathrm{g}})^{1/2} \tag{4}$$

where C_{m} [ms^{-1}] is the average speed of the piston and p_{g} – the instantaneous pressure of the gas. The p_{g} and T_{g} can be obtained from the 1-D combustion simulation.

The heat transfer at the top of the piston has a critical influence on the temperature distribution and heat load of the piston. The average temperature of the piston changes slowly, and it is basically constant in a working cycle [5]. Therefore, according to eqs. (5) and (6), the average in-cylinder gas temperature, T_{res}, in one cycle of the piston top surface and the average heat transfer coefficient, h_{gm}, are calculated:

$$T_{\mathrm{res}}=\frac{\int_0^{720} h_g T_g \mathrm{d}\varphi}{\int_0^{720} h_g \mathrm{d}\varphi} \tag{5}$$

$$h_{\mathrm{gm}} = \frac{\int_0^{720} h_g \mathrm{d}\varphi}{720} \tag{6}$$

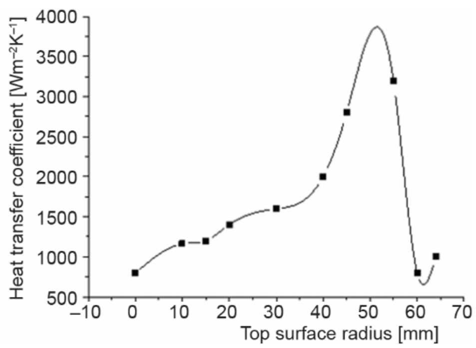

Figure 4. The h_{gm} of the top surface

The distribution of the average heat transfer coefficient at the top of the piston is not uniform and is usually related to the direction of fuel injection and the matching of the oil bundle and the combustion chamber. According to the calculation of in-cylinder combustion, the distribution of the average heat transfer coefficient in the radial direction of the piston top is shown in fig. 4. In order to avoid the fluid-solid coupling calculation of the heat transfer boundary with large workload, the similarity method of the average heat transfer coefficient distribution of the piston top is as follows. The average heat transfer coefficient of the top surface along the radial direction is proportional to its average temperature under different working conditions. This simplifies piston thermal load analysis at different operating conditions and environments.

The piston ring side is in contact with the cylinder liner, so the heat transfer coefficient and temperature distribution law of the cylinder liner side can be referred to [6]. The specific law is calculated:

$$h_{\mathrm{gm}}(h) = h_{\mathrm{gm}}(1 + k_1\beta)\mathrm{e}^{-\beta^{1/3}} \tag{7}$$

$$T_{\mathrm{gm}}(h) = T_{\mathrm{res}}(1 + k_2\beta)\mathrm{e}^{-\beta^{1/2}} \tag{8}$$

$$\beta = \frac{h}{S(0 \le \beta \le 1)} \tag{9}$$

$$k_1 = 0.573\left(\frac{S}{D}\right)^{0.24} \tag{10}$$

$$k_2 = 1.45k_1 \tag{11}$$

where h is the distance from the top of the cylinder liner, S – the piston stroke, D – the bore diameter, $h_{\mathrm{gm}}(h)$ – the average heat transfer coefficient of gas at the position of distance h, $T_{\mathrm{gm}}(h)$ – the average gas temperature at the position of distance h, β – the position ratio at distance h, k_1 – the corrected coefficient of heat transfer coefficient, and k_2 – the equivalent gas temperature correction factor. In this paper, k_1 is 0.589 and k_2 is 0.854.

The oscillating heat transfer of the piston is an unsteady two-phase flow problem. The fluid part contains organic oil and air, and the two are incompatible with each other, which will produce obvious boundaries. Therefore, the piston model is calculated by the VOF model. The VOF is a computational model in the Euler grid, and its phases cannot interpenetrate with each other, so it is suitable for fluid model calculation of multiphase flow [7]. The governing equations are:

$$\frac{\partial(\rho U)}{\partial t} + \nabla(\rho U \times U) = -\nabla P + \nabla(\mu\nabla \times U) + \rho \mathrm{g} + F \tag{12}$$

$$\frac{\partial \phi_q}{\partial t} + \nabla(U\phi_q) = 0 \tag{13}$$

$$\rho = \phi_{\mathrm{oil}}\rho_{\mathrm{oil}} + [1-\phi_{\mathrm{oil}}]\rho_{\mathrm{air}} \tag{14}$$

where μ is the dynamic viscosity coefficient, U – the fluid velocity, g – the gravitational acceleration, F – the volumetric force, ρ – the density, P – the pressure, and ϕ_{oil} – the proportion of oil.

According to the 1-D combustion software, the transient temperature and transient heat transfer coefficient in a cycle are averaged to obtain the average temperature, T_{res1}, in the cylinder and the average heat transfer coefficient, h_{gm1}, referring to eqs. (5) and (6). The calculation of the temperature field and heat transfer coefficient of the cooling side fluid is based on the initial value, so there is an error with the actual working conditions. Here, the fluid-solid iterative coupling method is used to eliminate the error. The cooling side analyzed by the oscillating heat transfer two-phase flow model is also a transient process, and the average value in one cycle of each node is calculated by eqs. (5) and (6). The cooling side average temperature, T_{res2}, and the average heat transfer coefficient, h_{gm2}, are mapped to the piston solid field, and T_{res2} and h_{gm2} are also mapped to the solid, so the complete temperature field of the piston is obtained. The piston temperature field is then mapped to the cooling side fluid field as a new initial condition, and the relevant parameters of the fluid field are recalculated. Iterate through this step until the front and rear iteration error of the piston at the same point is less than the set error of 1 °C. The logical process of this method is shown in fig. 5.

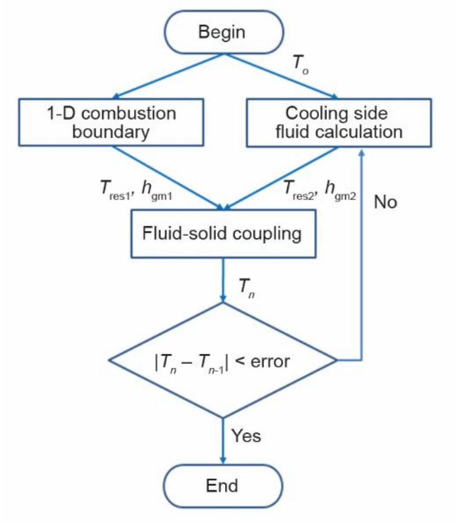

Figure 5. Temperture calculation flow chart

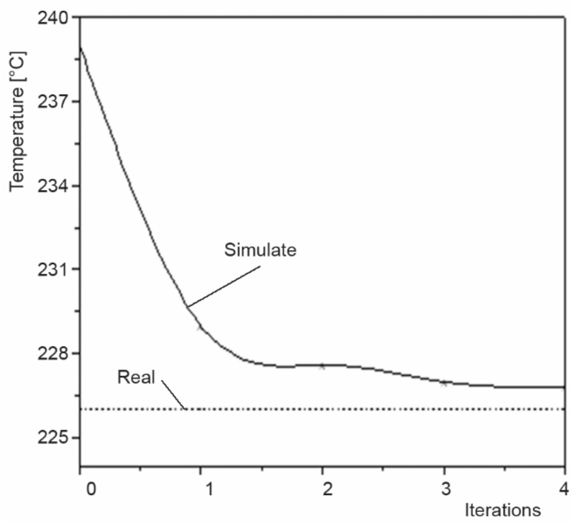

Figure 6. Iteration curve

Based on the calculation method of the three-coupling of the combustion side thermal boundary, the cooling side thermal boundary, and the piston solid field, the error caused by the initial temperature field calculation can be eliminated. Take a point at the piston ring groove as a reference point and then record the different temperatures of multiple iterations for this point. It can be seen from fig. 6 that this iterative method can analyze the temperature field more accurately.

Experiment analysis

In order to verify whether the above fluid-solid coupling model is realistic, the hardness plug measurement method is used to measure the temperature of each position of the piston. First, the holes are drilled at the critical position of the piston, and then the hardness plugs are placed in the hole. After the end of the experiment, the hardness plugs are polished, the hardness value is accurately measured by the hardness tester, and the corresponding temperature is determined by the calibration curve, and the obtained temperature is the temperature of the measured point. The specific measuring point position is shown in fig. 7.

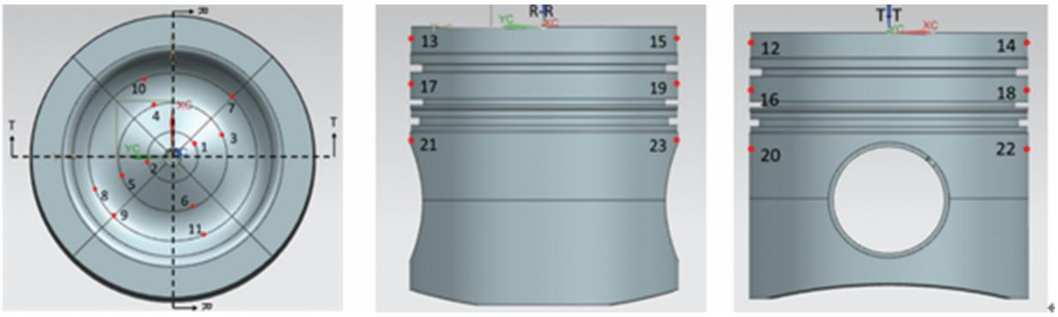

Figure 7. The distribution of the measurement points

The experimental point temperature and the simulated temperature pair are as shown in tab. 1. The inlet and outlet surfaces which will cause the different heat distribution of the top surface are not considered. Therefore, the simulation temperature is slightly lower than the experimental temperature as a whole, and the error is within 7%.

Table 1. The Comparison between Experiment and Simulation

No.	Real temperature [°C]	Simulated temperature [°C]	Error [%]	No.	Real temperature [°C]	Simulated temperature [°C]	Error [%]
1	343	340.9	0.6	13	283	267.9	5.3
2	366	352.6	3.9	14	288	268.6	6.7
3	302	287.1	4.9	15	288	287.3	0.2
4	311	302.2	2.8	16	171	173.1	1.2
5	330	307.9	6.7	17	175	169.3	3.2
6	292	296.5	1.5	18	156	162.1	3.9
7	355	333.2	6.1	19	176	166.5	5.4
8	308	311.5	1.1	20	131	138.4	5.6
9	328	322.7	1.6	21	136	129.1	5.1
10	330	320.6	2.8	22	156	146.9	5.8
11	333	327.9	1.5	23	163	157.8	3.2
12	288	278.1	3.4				

Analysis of influencing factors

Effect of air-fuel ratio

The air-fuel ratio in the cylinder has a direct influence on the combustion temperature in the cylinder, which in turn affects the thermal load of the piston. The working process simulation analysis of the performance for different supercharging systems is carried out, and the instantaneous pressure and temperature in the cylinder with the crank angle on the combustion side are obtained under different matching schemes, as shown in fig. 8. According to the similar relationship, the heat transfer coefficient distribution of the top surface can be obtained. The h_{gm2} and T_{res2} of the cooling side can be calculated by eqs. (5) and (6), and the thermal boundary conditions of the ring groove and bank can be obtained by eqs. (7)-(11).

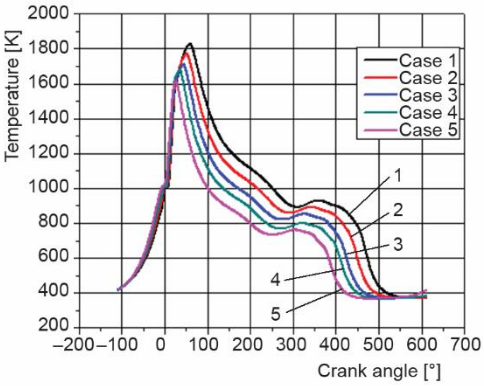

Figure 8. In-cylinder transient temperature in each case

According to the heat transfer boundary conditions under different cases, the maximum temperature of the top surface and the maximum temperature of the first ring groove are obtained by finite element calculation. It can be seen from fig. 9 that as the air-fuel ratio is reduced, the average temperature in the cylinder is increased, so that the maximum temperature at the top surface of the piston and the first ring groove is increased, and to a certain extent, a linear relationship.

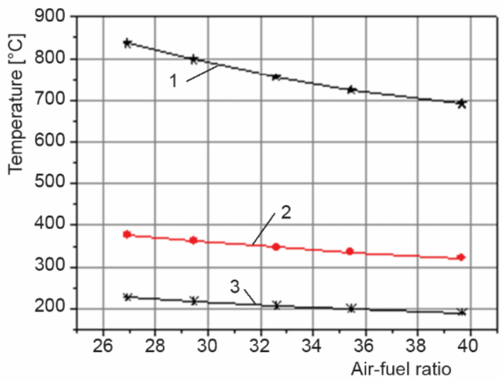

Figure 9. Temperature curve of different air-fuel cases; *1 – average temperature in the cylinder, 2 – maximal temperature of the piston head, and 3 – maximal temperature of the piston groove*

Effect of injection timing

Fuel injection timing has a critical impact on engine thermal load. When the other conditions are constant and the fuel injection is advanced, the in-cylinder pressure and the combustion temperature are increased, it means the heat load of the engine is increased. The working process simulation analysis of the performance of different start of injection angles is carried out, and the instantaneous pressure and temperature on the combustion side with the crank angle are obtained under different injection timings, as shown in fig. 10.

The method in section *Effect of air-fuel ratio* is also used to determine the piston heat transfer boundary conditions of different injection timing cases. The relationship between the maximum temperature of the piston top and the maximum temperature of the first ring groove is shown in fig. 11. It can be seen that the maximum temperature of the top surface of the piston and the maximum temperature of the first ring groove increase with the advance of the injection.

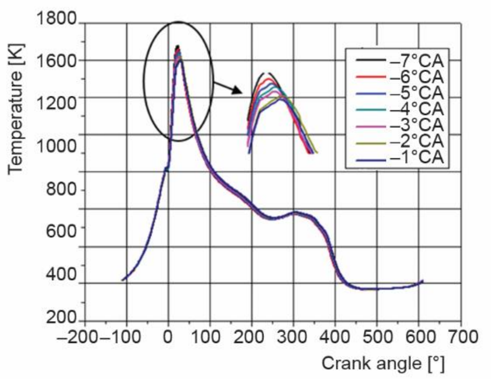

Figure 10. Transient temperature at different injecting time

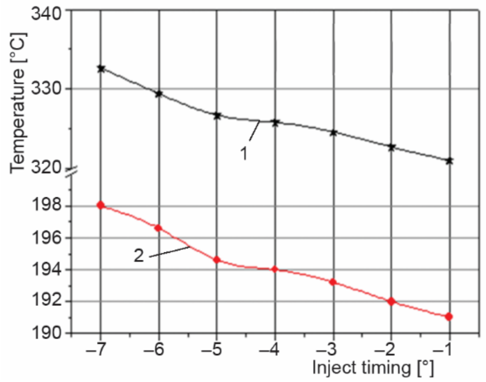

Figure 11. Maximum temperature at different position; *1 – maximal temperature of the piston head and 2 – maximal temperature of the piston groove*

Effect of filling rate

The filling rate is the percentage of the cooling oil to the total volume of the cooling chamber. The filling rate of the piston cooling inner cavity is determined by various factors, including the structure of cooling the inner cavity, the engine speed and the injection rate of the cooling oil, and the filling rate of the oil in the cooling inner cavity will greatly affect the heat exchange effect of the piston. It can be concluded from fig. 12 that with the up and down movement of the piston, the cooling oil shows a fluctuating state in the inner cavity, that is the oscillating heat exchange. As the injection velocity of the cooling oil increases, the filling rate also increases. As shown in fig. 13, as the engine speed increases, the filling rate of the oil decreases, and at different filling rates, the cooling effect in the piston cooling chamber is completely different.

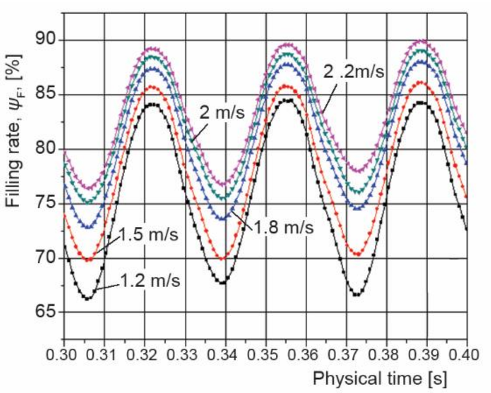

Figure 12. Filling rate at different injection velocities at 1800 rpm

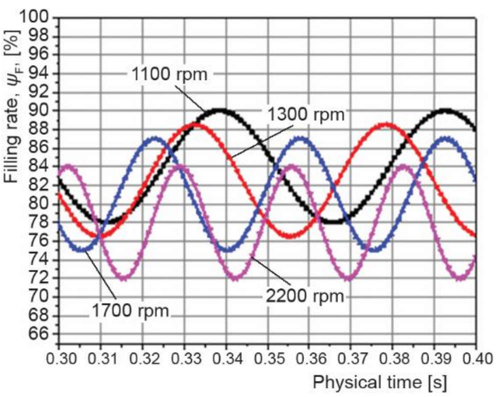

Figure 13. Filling rate at different engine speed

It can be seen from fig. 14 that the filling rate and cooling effect of the cooling oil are not proportional, and the larger the filling rate does not mean the better cooling effect. Here we select the maximum temperature of the top surface and the first ring groove as a criterion. As can be seen from the figure, if the piston filling rate is between 60% and 73.4%, with the increase of the oil filling rate, the effect of oscillating heat transfer is better, and the maximum temperature of each part of the piston is lowered. After the filling rate exceeds 73.4%, the effect of the oscillating heat transfer deteriorates with the further increase of the filling rate, resulting in an upward trend of the maximum temperature of the piston. This is because when the oil filling rate is too high or too low, it is impossible to form a good oscillating effect between the air and the cooling oil in the cooling inner cavity of the piston, so that the heat generated by the combustion cannot be taken away well.

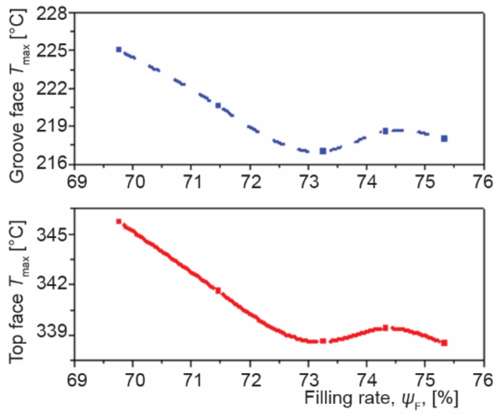

Figure 14. Maximum temperature at different filling rates

Prediction method

According to the previous analysis, the contour of the temperature field which is related to the air-fuel ratio, injection timing and filling rate is obtained, as seen in fig. 15.

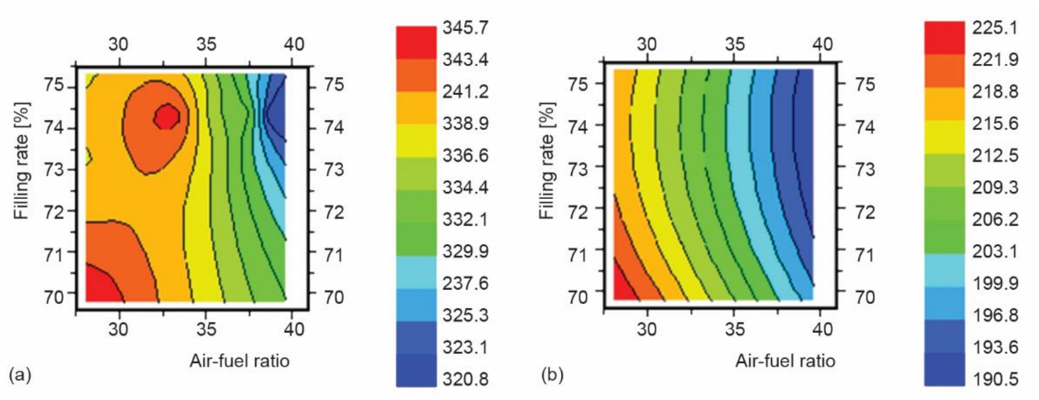

Figure 15. The T_{max} [°C] of the top surface (a) and the first groove surface (b)

When the temperature at the top of the piston is too high, the mechanical properties of the material are lowered, and the deformation resistance is also reduced. The lubrication condition of the piston ring is also affected by the heat load. Generally, the temperature of the first ring groove must be smaller than the glue temperature of the oil. From fig. 16, the operable area that meets the maximum temperature of the top surface and the first ring groove could be found.

The relationship between the piston thermal load and the injection air-fuel ratio, injection timing and filling rate is obtained, as shown in eqs. (15) and (16).

$$T_1 = -46.34x - 13.78y + 48.05z + 0.31x^2 + 0.073y^2 + 0.34z^2 - 1.22yz + 2478.85 \quad (15)$$

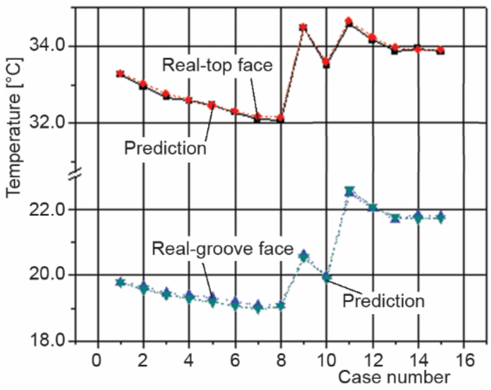

Figure 16. Error comparison

$$T_2 = -61.05x - 10.9y + 12.62z + 0.41x^2 + 0.1y^2 + 0.12z^2 - 0.33yz + 2734.2 \quad (16)$$

where T_1 is the maximum temperature of the piston top, T_2 – the maximum temperature of the first ring groove, x – the filling rate of the cavity, y – the air-fuel ratio in the cylinder, and z – the injection timing.

It can be concluded from fig. 16 that the prediction results obtained by eqs. (15) and (16) only have little error with the actual result, so the formula can well predict the maximum temperature of the top surface and the first ring groove surface. So according to the three factors above, the thermal load of this piston can be predicted during the designing process, which can greatly reduce the initial design time of the engine and also reduce the verification time for the thermal load reliability.

Acknowledgment

This project was completed with the help of teammates and also thanks to the help of the instructor.

Nomenclature

C_m – average piston speed, [ms^{-1}]
D – bore diameter, [m]
F – volumetric force, [N]
g – gravitational acceleration, [ms^{-2}]
h – distance from the top of the cylinder liner, [m]
h_g – instantaneous heat transfer coefficient of the gas, [Wm^{-2}K^{-1}]
h_{gm} – average heat transfer coefficient of the gas, [Wm^{-2}K^{-1}]
k_1 – corrected coefficient of heat transfer coefficient, [–]
k_2 – equivalent gas temperature correction factor, [–]
P – pressure, [Pa]
p_g – instantaneous pressure of the gas, [Pa]
q – heat transfer from gas to wall, [J]
S – piston stroke, [m]
t – time, [s]
$t_{w,s}$ – instantaneous temperature of the top surface, [K]
T_{res} –average gas temperature of the gas, [K]
T_{wm}– average temperature of the wall, [K]
T_1 – maximum temp of the top surface, [°C]
T_2 – maximum temp of the first groove surface, [°C]
T_g – instantaneous temperature of the gas, [K]
U – fluid velocity, [ms^{-1}]
x – filling rate of the cavity, [%]
y – air-fuel ratio, [–]
z – injecting timing, [–]

Greek symbols

β – position ratio at distance h, [–]
μ – dynamic viscosity coefficient, [Nsm^{-2}]
ρ – density, [kgm^{-3}]
ϕ_{oil} – proportion of oil, [–]

References

[1] Liu, X. F., *et al.*, Finite Element Analysis of Thermo-Mechanical Conditions Inside the Piston of a Diesel Engine, *Applied Thermal Engineering*, *119* (2017), 2, pp. 312-318
[2] Meng, F. M., *et al.*, Thermo-Elasto-Hydrodynamic Lubrication Analysis of Piston Skirt Considering Oil Film Inertia Effect, *Tribology International*, *40* (2007), 7, pp. 1089-1099
[3] Lu, X., *et al.*, Thermal Analysis on pIston of Marine Diesel Engine, *Applied Thermal Engineering*, *50* (2013), 1, pp. 168-176
[4] Pan, J., *et al.*, 3-D Modeling of Heat Transfer in Diesel Engine Piston Cooling Galleries, SAE Technical paper 2005-01-1644, 2005

[5] Esfahanian, V., *et al.*, Thermal Analysis of an SI Engine Piston Using Different Combustion Boundary Condition Treatments, *Applied Thermal Engineering*, *26* (2006), 2, pp. 277-287
[6] Hun, Z., Reitz, R. D., A Temperature Wall Function Formulation for Variable-Density Turbulent Flows with Application to Engine Convective Heat Transfer Modeling, *International Journal of Heat and Mass Transfer*, *40* (1997), 3, pp. 613-625
[7] Abbassi, W., *et al.*, Numerical Simulation of Free Ascension and Coaxial Coalescence of Air Bubbles Using the Volume of Fluid Method (VOF), *Computers & Fluids*, *161* (2018), Jan., pp. 47-59

Paper submitted: September 15, 2019
Paper revised: April 4, 2020
Paper accepted: April 5, 2020